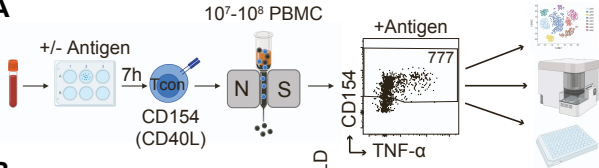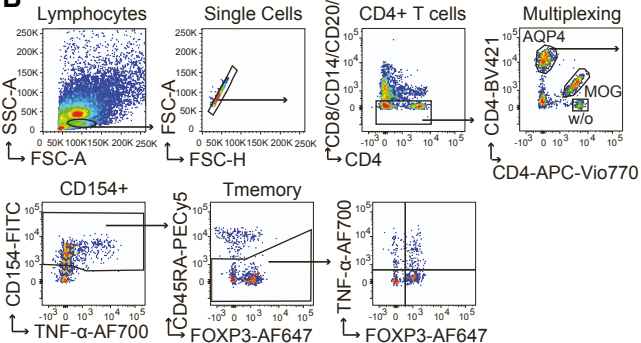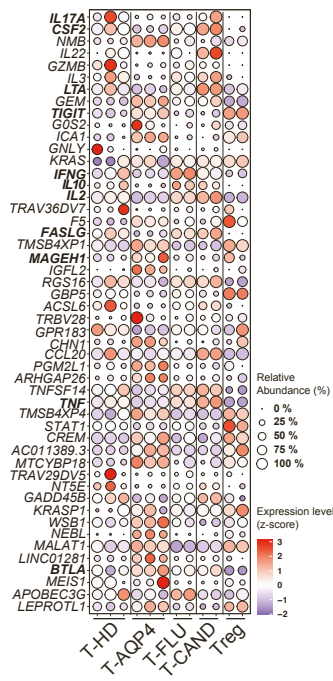## Supplemental information

# Autoantigen-specific CD4+ T cells acquire

# an exhausted phenotype and persist in human
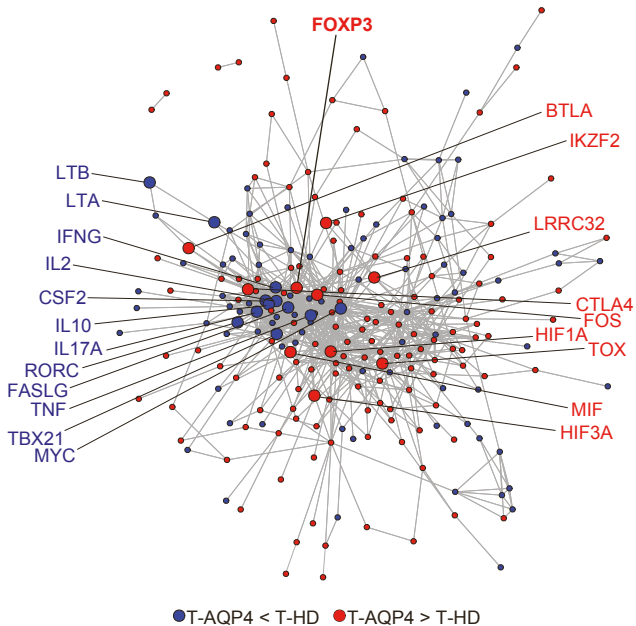
# antigen-specific autoimmune diseases

Carina Saggau, Petra Bacher, Daniela Esser, Mahdi Rasa, Silja Meise, Nicola Mohr, Nora Kohlstedt, Andreas Hutloff, Sarah-Sophie Schacht, Justina Dargvainiene, Gabriela Rios Martini, Klarissa H. Stürner, Ina Schröder, Robert Markewitz, Johannes Hartl, Maria Hastermann, Ankelien Duchow, Patrick Schindler, Mareike Becker, Carolin Bautista, Judith Gottfreund, Jörn Walter, Julia K. Polansky, Mingxing Yang, Reza Naghavian, Mareike Wendorff, Ev-Marie Schuster, Andreas Dahl, Andreas Petzold, Susanne Reinhardt, Andre Franke, Marek Wieczorek, Lea Henschel, Daniel Berger, Guido Heine, Maike Holtsche, Vivien Häußler, Christian Peters, Enno Schmidt, Simon Fillatreau, Dirk H. Busch, Klaus-Peter Wandinger, Kilian Schober, Roland Martin, Friedemann Paul, Frank Leypoldt, and Alexander Scheffold

**A**

+/- Antigen

7h

Tcon
CD154
(CD40L)

$10^7$-$10^8$ PBMC

N  S

+Antigen

777

CD154

TNF-α

**B**

Lymphocytes

SSC-A

FSC-A

Single Cells

FSC-A

FSC-H

CD4+ T cells

CD8/CD14/CD20/LD

CD4

Multiplexing

CD4-BV421

AQP4

MOG

w/o

CD4-APC-Vio770

CD154+

CD154-FITC

TNF-α-AF700

Tmemory

CD45RA-PECy5

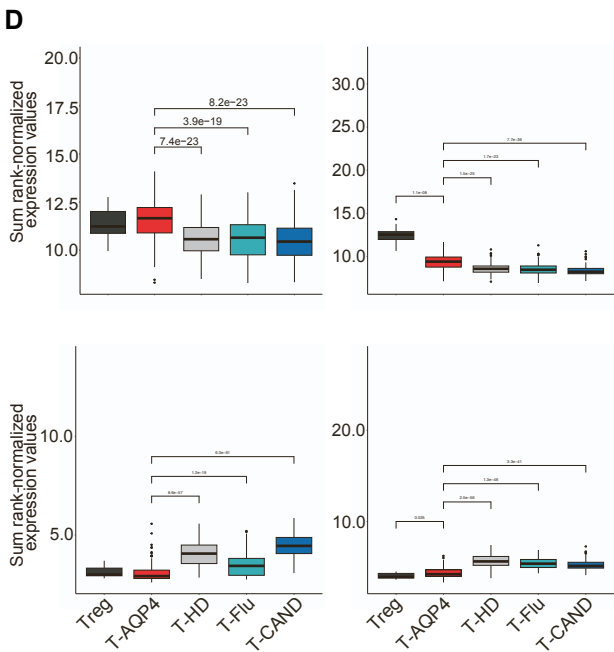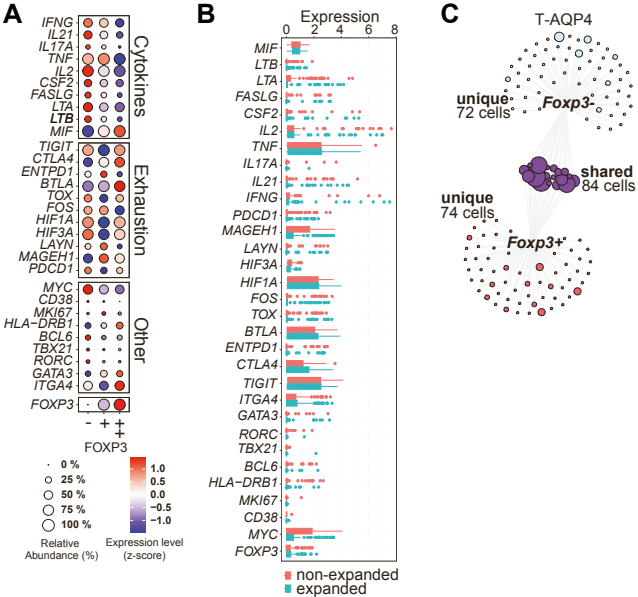FOXP3-AF647

TNF-α-AF700

FOXP3-AF647

**Supplemental Figure 1: Antigen-reactive T cell enrichment (ARTE), related to Figures 1-6. (A)** Schematic of ARTE: PBMCs were stimulated with or without AQP4 or MOG peptide pools for 7 hours and reactive T cells were detected according to upregulation of CD154 (CD40L). CD154+ cells were magnetically enriched from 25-50 million PBMCs. Dotplot example shows AQP4-reactive CD154+ cells after magnetic enrichment. Absolute cell count of CD154+ isolated from 50 million PBMCs is indicated. Figure created with Biorender.com. **(B)** Gating strategy of AQP4-reactive T cells detected by ARTE including multiplexing of differently stimulated samples (w/o antigen, MOG, AQP4). For Multiplexing cells were labeled with different CD4-antibodies and mixed.

**A**

IL17A
CSF2
NMB
IL22
GZMB
IL3
LTA
GEM
TIGIT
G0S2
ICA1
GNLY
KRAS
IFNG
IL10
IL2
TRAV36DV7
F5
FASLG
TMSB4XP1
MAGEH1
IGFL2
RGS16
GBP5
ACSL6
TRBV28
GPR183
CHN1
CCL20
PGM2L1
ARHGAP26
TNFSF14
TNF
TMSB4XP4
STAT1
CREM
AC011389.3
MTCYBP18
TRAV29DV5
NT5E
GADD45B
KRASP1
WSB1
NEBL
MALAT1
LINC01281
BTLA
MEIS1
APOBEC3G
LEPROTL1

T-HD  T-AQP4  T-FLU  T-CAND  Treg

**Relative Abundance (%)**
· 0 %
○ 25 %
○ 50 %
○ 75 %
○ 100 %

**Expression level (z-score)**
3
2
1
0
-1
-2

**B** Protein interaction network

**FOXP3**

LTB
LTA
IFNG
IL2
CSF2
IL10
IL17A
RORC
FASLG
TNF
TBX21
MYC

BTLA
IKZF2
LRRC32
CTLA4
FOS
HIF1A
TOX
MIF
HIF3A

● T-AQP4 < T-HD   ● T-AQP4 > T-HD

**Supplemental Figure 2: Top50 differentially expressed genes between T-AQP4 and T-HD and protein network interaction analysis, related to Figure 2. (A)** Bubble plot showing the normalized expression of the Top50 differentially expressed genes of AQP4-reactive CD154+ T cells between healthy donors (T-HD; n=3) and AQP4-NMOSD patients (T-AQP4; n=3) according to fold change (adjusted p-values <0.05). Normalized expression of the same genes of *Influenza-* (T-FLU; n=2) and *C. albicans*-specific T cells (T-CAND; n=2) as well as polyclonally activated Tregs (Treg; n=2) were plotted as control. The size of the bubble shows the proportion of cells expressing the respective gene, and the colors show the relative average expression of the genes in all the cells belonging to each group. **(B)** Undirected bioinformatic protein network analysis based on all differentially expressed genes between healthy donors (T-HD) and AQP4-NMOSD patients (T-AQP4).

**A**

Cytokines: IFNG, IL21, IL17A, TNF, IL2, CSF2, FASLG, LTA, **LTB**, MIF

Exhaustion: TIGIT, CTLA4, ENTPD1, BTLA, TOX, FOS, HIF1A, HIF3A, LAYN, MAGEH1, PDCD1

Other: MYC, CD38, MKI67, HLA−DRB1, BCL6, TBX21, RORC, GATA3, ITGA4

FOXP3

FOXP3   −  +  ++

Relative Abundance (%): 0 %, 25 %, 50 %, 75 %, 100 %

Expression level (z-score): 1.0, 0.5, 0.0, −0.5, −1.0

**B**

Expression: 0, 2, 4, 6, 8

MIF, LTB, LTA, FASLG, CSF2, IL2, TNF, IL17A, IL21, IFNG, PDCD1, MAGEH1, LAYN, HIF3A, HIF1A, FOS, TOX, BTLA, ENTPD1, CTLA4, TIGIT, ITGA4, GATA3, RORC, TBX21, BCL6, HLA−DRB1, MKI67, CD38, MYC, FOXP3

non-expanded
expanded

**C**

T-AQP4

unique 72 cells

*Foxp3*−

shared 84 cells

unique 74 cells

*Foxp3*+

**D**

Sum rank-normalized expression values

7.4e−23
3.9e−19
8.2e−23

1.1e−08
1.7e−22
7.7e−06

8.8e−37
8.2e−01

0.035
2.5e−08
1.3e−08
3.3e−47

Treg, T-AQP4, T-HD, T-Flu, T-CAND

**Supplemental Figure 3: Developmental trajectory of ThEx cells supported by TCR clonality data, related to Figure 2. (A)** Bubble plot showing the normalized expression of selected marker genes in AQP4-reactive CD154+ T cells of AQP4-NMOSD patients (T-AQP4; n=3) according to their normalized expression of *FOXP3* (*FOXP3*- (-), *FOXP3* intermediate (+) *FOXP3* high (++). The size of the bubble shows the proportion of cells expressing the respective gene, and the colors show the relative average expression of the genes in all the cells belonging to each group. **(B)** Box plots showing the normalized expression of selected marker genes comparing clonally expanded (clone frequency>1) and non-expanded (clone frequency=1) T cell receptors within T-AQP4 cells. **(C)** T cell receptor (TCR) network plot of AQP4-reactive CD154+ T cells from AQP4-NMOSD patients (T-AQP4; n=3) comparing the TCRs of *FOXP3*+ and *FOXP3*- AQP4-reactive T cells. Each node indicates one TCR clone. The size of the node shows the TCR clonality. Blue color indicates uniquely *FOXP3*- TCRs, pink color indicates uniquely *FOXP3*+ TCRs and purple color indicates TCRs shared between *FOXP3*+ and *FOXP3*-. **(D)** Gene signature analysis: boxplots comparing AQP4-reactive CD154+ T cells from NMOSD patients (T-AQP4; n=3) and healthy donors (T-HD; n=3) with *C. albicans*-reactive T cells (T-CAND; n=2), *Influenza*-reactive T cells (T-Flu; n=2) and polyclonally activated CD137+ Tregs (Treg; n=2). Shown is the sum of rank normalized expression values based on 4 selected gene groups representing the different Th subset signatures (Tfh, Treg, Th1, Th17).
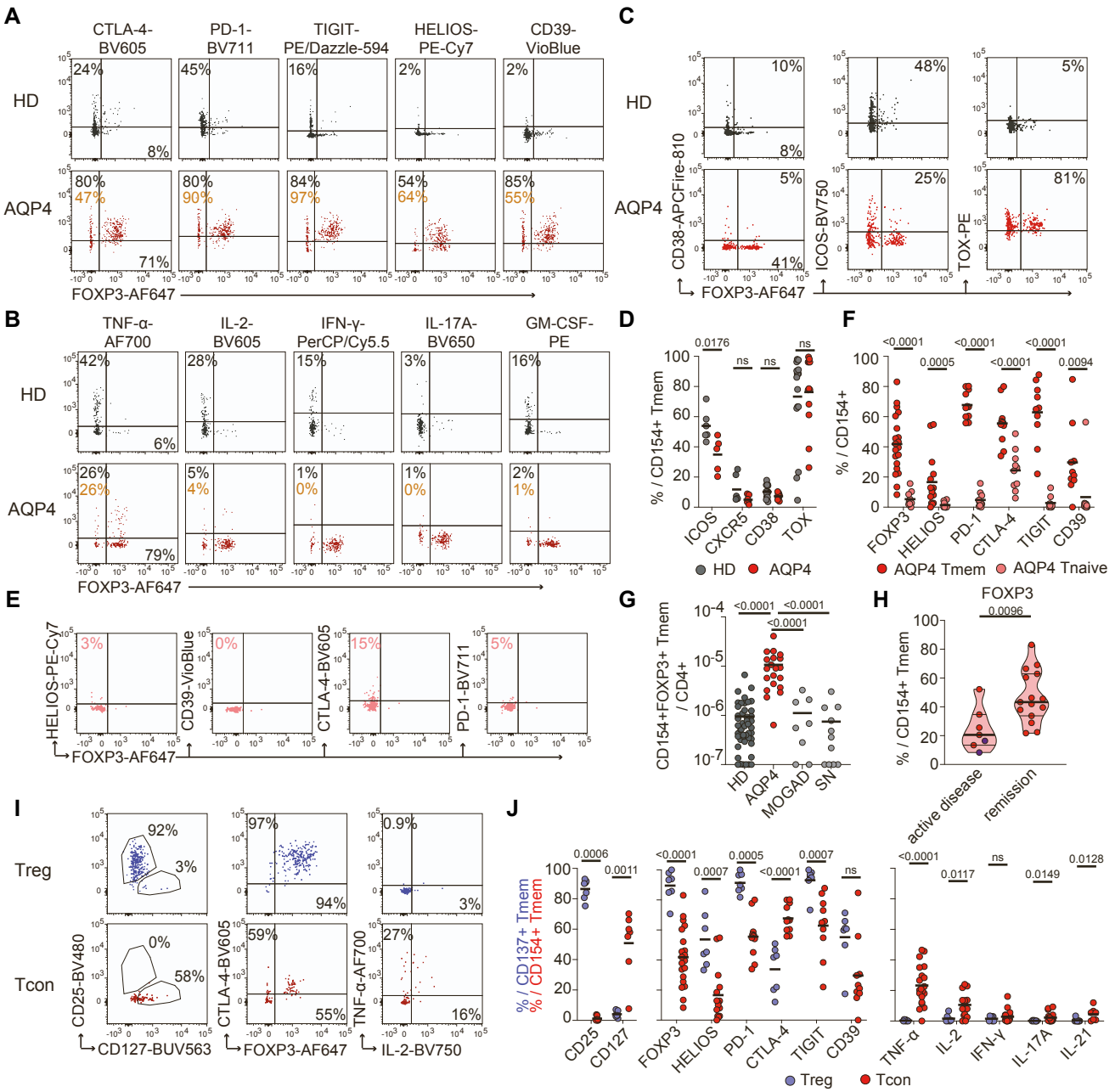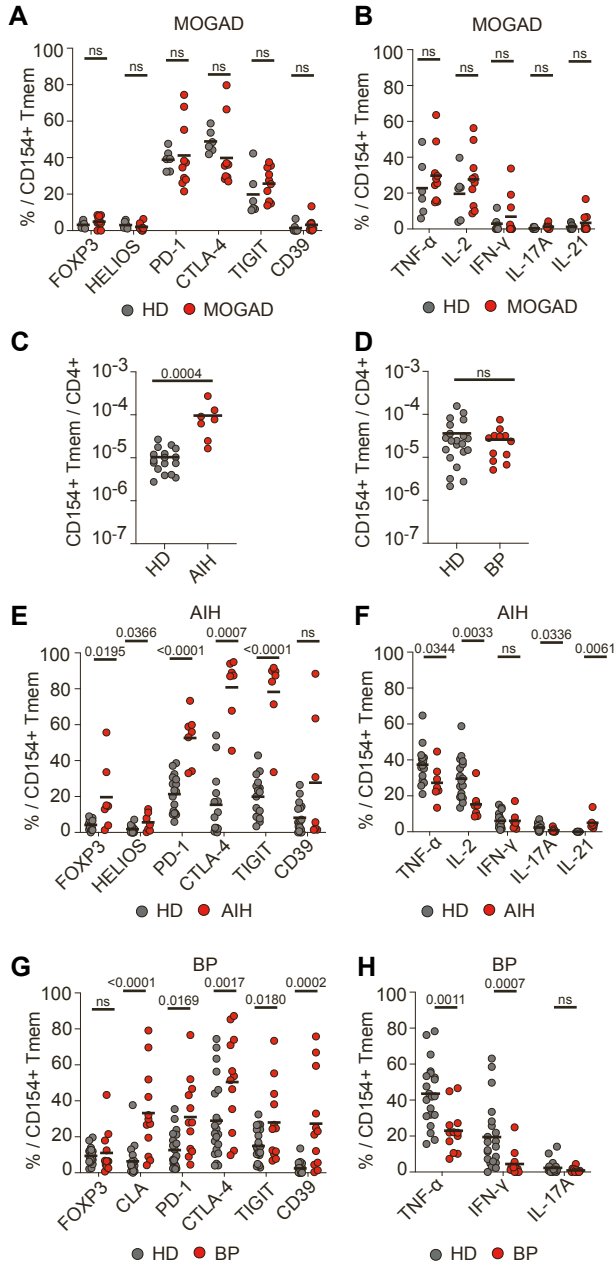
**Supplemental Figure 4: Flow cytometric analysis of AQP4-reactive CD4+ T cells following ARTE, related to Figure 3.** Dotplot examples of **(A)** *ex vivo* co-inhibitory receptor (CTLA-4, PD-1, TIGIT), FOXP3, HELIOS and CD39 or **(B)** *ex vivo* cytokine expression by AQP4-reactive CD154+ Tmem in healthy donors (HD) and AQP4-NMOSD patients (AQP4) detected by ARTE. Percentages of cells within all CD154+Tmem (black) and within CD154+FOXP3+ Tmem (orange) are indicated. **(C)** Dotplot examples of *ex vivo* expression of chronic activation markers CD38 and ICOS and transcription factor TOX by AQP4-reactive CD154+ Tmem in healthy donors (HD) and AQP4-NMOSD patients (AQP4) detected by ARTE. **(D)** Proportion of ICOS, CXCR5, CD38 and TOX expression within AQP4-reactive CD154+ Tmem in healthy donors (HD; n=6-17) and AQP4-NMOSD patients (AQP4; n=5-12). **(E)** Dotplot examples of *ex vivo* expression of HELIOS, CD39, CTLA-4 and PD-1 of AQP4-reactive naïve CD154+ T cells detected by ARTE. Percentage within naïve CD154+ T cells is indicated. **(F)** Comparison between CD45RA+ naïve (Tnaive; n=10) and CD45RA- memory (Tmem; n=11-20) CD154+ T cells in AQP4-NMOSD patients (AQP4). **(G)** Frequencies of AQP4-reactive CD154+FOXP3+CD45RA- memory (Tmem) CD4+ T cells in healthy donors (HD; n=48) and NMOSD patients n=39 (AQP4; n=20, MOG antibody-associated disease (MOGAD); n=8, seronegative (SN); n=11). **(H)** Proportion of FOXP3 expression within AQP4-reactive CD154+ Tmem from AQP4-NMOSD patients according to their clinical status, active disease (n=7, new onset, or relapse, <3 month since last disease flare, one patient was measured twice during active disease indicated by purple color of the dots) and stable remission (n=15). **(I)** Dotplot examples of *ex vivo* CD25, CD127, CTLA-4, FOXP3, IL-2 and TNF-$\alpha$ expression by AQP4-reactive CD154+ Tmem (Tcon) and CD137+ Tmem (Tregs) in AQP4-NMOSD patients detected by ARTE. Percentages of cells within all CD154+ Tcon and CD137+ Tregs are indicated. **(J)** *Ex vivo* proportion of CD25, CD127, FOXP3, HELIOS, co-inhibitory receptor (CTLA-4, PD-1, TIGIT) and CD39 as well as cytokine (TNF-$\alpha$, IL-2, IFN-$\gamma$, IL-17A, IL-21) expressing cells within AQP4-reactive CD154+ Tmem and CD137+ Tmem in AQP4-NMOSD patients (Tcon; n=7-20, Treg; n=7). Each symbol in **(D, F, G, H, J)** represents one donor, horizontal lines indicate mean. Truncated violin plots with quartiles and range are shown in **(H)**. Statistical differences: Two-tailed Mann-Whitney test or unpaired t test in **(D, F, G, H, J)**. Decision was based on an upstream normal distribution test.

**A**

**B**

**C**

**D**

**E**

**F**

**G**

**H**
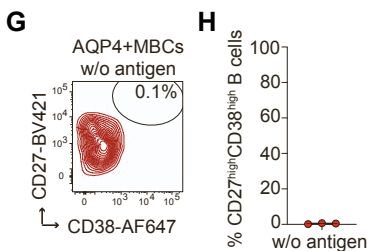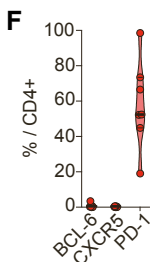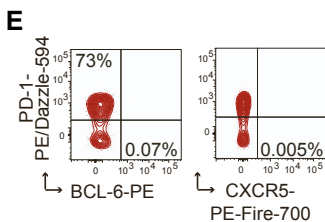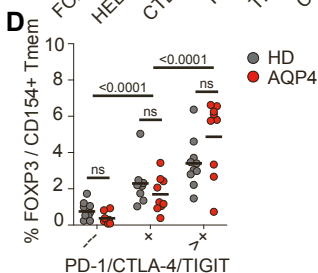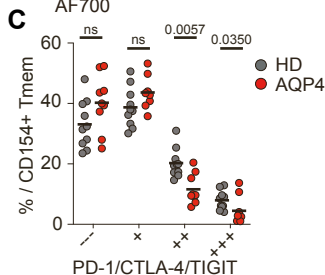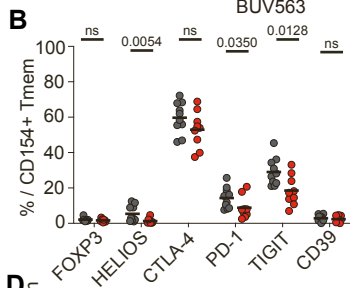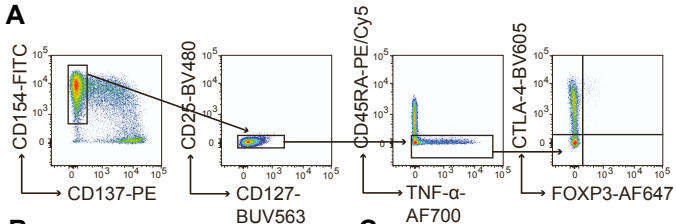
**Supplemental Figure 5: Low frequencies of ThEx cells can be found upon polyclonal stimulation of CD4 memory T cells in healthy donors and NMOSD patients and T cell/B cell cooperation assay, related to Figure 4. (A)** Gating strategy of PMA and Ionomycin activated CD4 memory T cells. **(B)** *Ex vivo* proportion of FOXP3, HELIOS, co-inhibitory receptor (CTLA-4, PD-1, TIGIT) and CD39 expressing cells within polyclonally activated CD154+ Tmem from healthy donors (HD; n=10) and AQP4-NMOSD patients (AQP4; n=9). **(C)** *Ex vivo* proportion of cells expressing none, single, double, or triple co-inhibitory receptors (CTLA-4, PD-1 or TIGIT) within polyclonally activated CD154+ Tmem in healthy donors (HD; n=10) and AQP4-NMOSD patients (AQP4; n=9) **(D)** Proportion of FOXP3 positive polyclonally activated CD154+ Tmem from healthy donors (HD; n=10) and AQP4-NMOSD patients (AQP4; n=9) expressing none, single or >1 co-inhibitory receptor (PD-1, CTLA-4 or TIGIT). **(E)** Contour plot examples of TfH marker (PD-1, CXCR5, BCL-6) expression of expanded AQP4-reactive T cell clones. Percentages within CD4+ T cells are indicated. **(F)** Proportion of TfH marker (BCL-6, CXCR5, PD-1) expression within CD4+ T cells of expanded AQP4-reactive T cell clones (n=7). **(G)** Contour plot example of CD27 and CD38 staining showing the co-culture of one AQP4-reactive T cell clone with heterologous memory B cells in absence of the antigen (AQP4). Percentage of CD27$^{high}$CD38$^{high}$ plasmablasts is indicated. **(H)** Proportion of CD27$^{high}$CD38$^{high}$ memory B cells co-cultured with AQP4-reactive T cells clones in absence of the antigen (AQP4) (n=3). Each symbol in **(B, D)** represents one T cell clone. Truncated violin plots with quartiles and range are shown in **(B)**. Each symbol in **(B-D)** represents one donor, horizontal lines indicate mean. Statistical differences: Two-tailed Mann-Whitney test or unpaired t test in **(B-D)**. Decision was based on an upstream normal distribution test. Each symbol in **(F, H)** represents one T cell clone. Truncated violin plots with quartiles and range are shown in **(F)**.

**A** MOGAD

% / CD154+ Tmem

ns ns ns ns ns ns

FOXP3 HELIOS PD-1 CTLA-4 TIGIT CD39

● HD ● MOGAD

**B** MOGAD

% / CD154+ Tmem

ns ns ns ns ns

TNF-α IL-2 IFN-γ IL-17A IL-21

● HD ● MOGAD

**C**

CD154+ Tmem / CD4+

0.0004

HD AIH

**D**

CD154+ Tmem / CD4+

ns

HD BP

**E** AIH

% / CD154+ Tmem

0.0366
0.0195    <0.0001    0.0007    <0.0001    ns

FOXP3 HELIOS PD-1 CTLA-4 TIGIT CD39

● HD ● AIH

**F** AIH

% / CD154+ Tmem

0.0344    0.0033    ns    0.0336    0.0061

TNF-α IL-2 IFN-γ IL-17A IL-21

● HD ● AIH

**G** BP

% / CD154+ Tmem

ns    <0.0001    0.0169    0.0017    0.0180    0.0002

FOXP3 CLA PD-1 CTLA-4 TIGIT CD39

● HD ● BP

**H** BP

% / CD154+ Tmem

0.0011    0.0007    ns

TNF-α IFN-γ IL-17A

● HD ● BP

**Supplemental Figure 6: Flow cytometric analysis of SLA-, BP180- and MOG-reactive CD4+ T cells following ARTE, related to Figure 5.** *Ex vivo* cytometric characterization of SLA-, BP180- and MOG-reactive CD154+ T cells following ARTE. **(A)** *Ex vivo* proportion of FOXP3, HELIOS, co-inhibitory receptor (CTLA-4, PD-1, TIGIT) and CD39 expressing cells within MOG-reactive CD154+ Tmem from healthy donors (HD; n=) and MOGAD patients (MOGAD; n=). **(B)** *Ex vivo* Cytokine expression (TNF-$\alpha$, IL-2, IFN-$\gamma$, IL-17A, IL-21) of MOG-reactive CD154+ Tmem in healthy donors (HD; n=6) and MOGAD patients (MOGAD; n=10). **(C)** Frequencies of SLA-reactive CD154+CD45RA- memory CD4+ T cells (Tmem) in healthy donors (HD; n=17) and AIH patients (n=7). **(D)** Frequencies of BP180-reactive CD154+CD45RA- memory CD4+ T cells (Tmem) in healthy donors (HD; n=21) and BP patients (n=12). **(E)** *Ex vivo* proportion of FOXP3, HELIOS, co-inhibitory receptor (CTLA-4, PD-1, TIGIT) and CD39 expressing cells within SLA-reactive CD154+ Tmem from healthy donors (HD; n=14-17) and AIH patients (AIH; n=7). **(F)** *Ex vivo* Cytokine expression (TNF-$\alpha$, IL-2, IFN-$\gamma$, IL-17A, IL-21) of SLA-reactive CD154+ Tmem in healthy donors (HD; n=4-17) and AIH patients (AIH; n=7). **(G)** *Ex vivo* proportion of FOXP3, CLA, co-inhibitory receptor (CTLA-4, PD-1, TIGIT) and CD39 expressing cells within BP180-reactive CD154+ Tmem from healthy donors (HD; n=21) and BP patients (BP; n=12). **(H)** *Ex vivo* Cytokine expression (TNF-$\alpha$, IFN-$\gamma$, IL-17A) of BP180-reactive CD154+ Tmem in healthy donors (HD; n=21) and BP patients (BP; n=12). Each symbol in **(A-H)** represents one donor, horizontal lines indicate mean. Statistical differences: Two-tailed Mann-Whitney test or unpaired t test in **(A-H)**. Decision was based on an upstream normal distribution test.
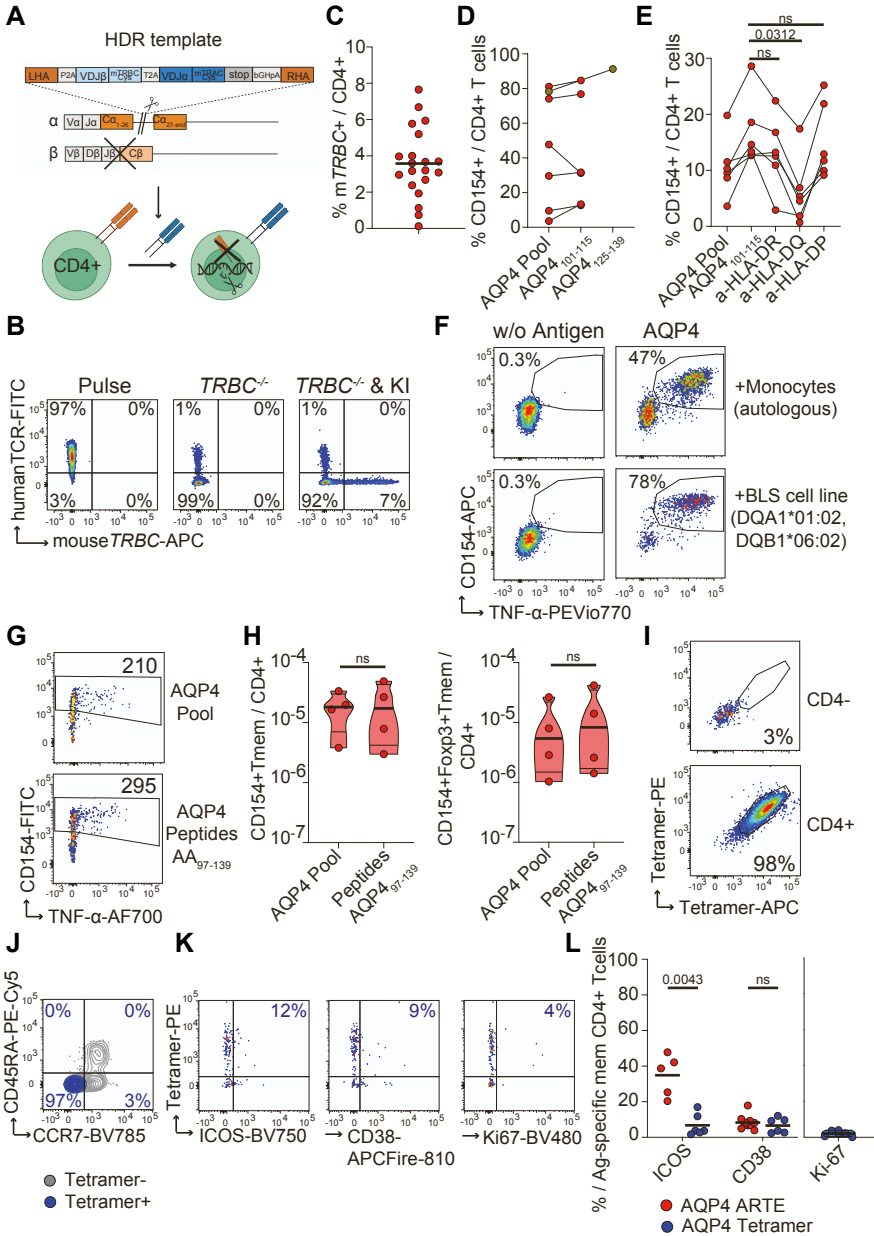
**Supplemental Figure 7: Identification of immunodominant AQP4 epitopes in NMOSD patients via orthotopic T cell receptor (TCR) replacement, related to Figure 6.**

**(A)** Schematic of the TCR replacement including the homology-directed repair (HDR) template design: The HDR template comprises the full length of the $\alpha$- and $\beta$-chains of the inserting TCRs flanked by left and right homology arms (LHA and RHA) and contains self-cleaving peptides (P2A and T2A), as well as a poly-A tail (bGHpA). The $\beta$-chain consists of the human variable region and the murine constant region, which is used as tracking marker. Clonally expanded TCRs from three AQP4-NMOSD patients were re-expressed via orthotopic TCR replacement using CRISPR/Cas9 knock-in into the *TCRA*-locus of primary CD4+ T cells, and simultaneous *TCRB*-locus$^{-/-}$ leading to exclusive expression of the transgenic TCR. Figure created with Biorender.com. **(B)** Dotplot examples of human and mouse TCR staining in TCR-transgenic cells of the pulse control, the *TCRB*$^{-/-}$ only control of the endogenous TCR and the simultaneous *TCRB*$^{-/-}$ of the endogenous TCR and Knock-in (KI) of the AQP4-specific transgenic TCR. The transgenic TCRs consist of the human variable region and the murine constant region. **(C)** Proportion of mouse TRBC+CD4+ T cells after TCR replacement via CRISPR/Cas9 shown for all TCRs replaced from 3 AQP4-NMOSD patients (n=20). **(D)** Identification of two immunodominant peptides (AQP4$_{101-115}$ and AQP4$_{125-139}$) in one AQP4-NMOSD patient by restimulation of TCR-transgenic T cells (n=7) with the AQP4 peptide pool and single peptides covering the complete protein sequence. **(E)** Proportion of CD154+ T cells of expanded AQP4-specific TCR-transgenic cells (n=6) of one AQP4-NMOSD patient restimulated with the whole AQP4 peptide pool or the identified immunodominant peptide (AQP4$_{101-115}$) with and without HLA blocking antibodies. **(F)** Dotplot examples of the restimulation of AQP4-reactive T cell clones in presence of autologous monocytes or DQw6 BLS cells. Percentages of CD154+TNF-$\alpha$+ T cells are indicated. **(G)** Dotplot examples of the *ex vivo* detection of AQP4-reactive CD4+ T cells by ARTE. Absolute cell counts after magnetic enrichment from $2.5\times10^7$ PBMCs stimulated with the whole AQP4 peptide pool or a selection of six peptides are indicated. **(H)** Comparison of frequencies of AQP4-reactive CD154+ Tmem and CD154+FOXP3+ Tmem in HLA-DQ6+ AQP4-NMOSD patients (n=4) stimulated with the whole AQP4 peptide pool versus six selected peptides (AQP4$_{97-139}$). **(I)** Dotplot examples of tetramer staining of TCR-transgenic CD4+ T cells. Percentage of tetramer+ cells within CD4+ and CD4- T cells is indicated. **(J)** Contour plot example of CD45RA and CCR7 staining of antigen-specific CD4+ T cells detected via tetramer enrichment overlaid with two different colors representing tetramer APC/PE double positive cells (blue) and tetramer- cells (grey). **(K)** Dotplot examples of antigen-specific CD4+ T cells in AQP4-NMOSD patients detected by tetramer enrichment. Percentages of cells within tetramer APC/PE double positive cells are indicated. **(L)** Comparison of the proportion of ICOS, CD38 and Ki-67 expression within antigen-specific CD4+ T cells detected by ARTE or tetramer enrichment in AQP4-NMOSD patients (AQP4 ARTE; n=5-10, AQP4 tetramer; n=6). For Ki-67 no ARTE data is available. Each symbol in **(H, L)** represents one donor. Each symbol in **(C, D, E)** represents one replaced TCR. Horizontal lines indicate mean. Truncated violin plots with quartiles and range are shown in **(H)**. Statistical differences: Two-tailed Mann-Whitney test in **(E, H, L)**.